Strain-dependent modifier genes determine survival in *Zfp423* mice

Wendy A. Alcaraz, Zheng Liu, Phoebe Valdes, Edward Chen,
Alan G. Valdovino Gonzalez, Shelby Wade, Cinny Wong, Eunnie Kim, Hsiang-Hua M. Chen, Dorothy Concepcion, and Bruce A. Hamilton*

Biomedical Sciences Graduate Program,
Department of Cellular & Molecular Medicine,
Department of Medicine,
UC San Diego Moores Cancer Center, and
Institute for Genomic Medicine
University of California, San Diego
La Jolla, CA 92093

* Author for correspondence: bah@ucsd.edu

Current addresses:
W.A.A.: Ambry Genetics, Aliso Viejo, CA
Z.L.: GenScript USA Inc, San Francisco, CA
P.V.: Bioengineering Graduate Program, University of California, San Diego, CA
E.C.: Taipei Medical University Hospital, Taipei, Taiwan ROC
A.G.V.G: Department of Orthopedic Surgery, University of California, San Diego, CA

ORCIDs:
Zheng Liu 0000-0002-7883-9346
Phoebe Valdes 0000-0003-3165-7235
Edward Chen 0000-0003-0558-3703
Alan G. Valdovino Gonzalez 0000-0003-1974-4782
Shelby Wade 0000-0001-7833-2580
Cinny Wong 0000-0002-9542-5743
Eunnie Kim 0000-0002-7641-933X.
Hsiang-Hua M. Chen 0000-0001-7125-6888
Dorothy Concepcion 0000-0002-8506-1229
Bruce A. Hamilton 0000-0001-5599-9139

ABSTRACT

Zfp423 **encodes a transcriptional regulatory protein that interacts with canonical signaling and lineage pathways. Mutations in mouse** ***Zfp423*** **or its human ortholog** ***ZNF423*** **are associated with a range of developmental abnormalities reminiscent of ciliopathies, including cerebellar vermis hypoplasia and other midline brain defects. Null mice have reduced viability in most strain backgrounds. Here we show complete lethality on a C57BL/6J background, dominant rescue in backcrosses to any of 13 partner strains, with strain-dependent survival frequencies, and evidence for a BALB/c-derived survival modifier locus on chromosome 5. Survival data indicate both perinatal and postnatal periods of lethality. Anatomical data from a hypomorphic gene trap allele observed on both C57BL/6J and BALB/c congenic backgrounds shows an aggregate effect of background on sensitivity to Zfp423 loss rather than a binary effect on viability.**

Introduction

Zfp423 and its human homolog ZNF423 are transcriptional regulators that intersect both lineage and signal-induced pathways. Zfp423 was first described as an inhibitory interacting factor for Ebf-family basic helix-loop-helix (bHLH) transcription factors, blocking Ebf-dependent development in olfactory neurogenesis [1-3]. Zfp423 was later independently found as a binding partner of BMP-dependent SMAD transcription factors [4], retinoic acid receptors [5], cleaved Notch intracellular domain [6] and DNA damage response proteins [7]. Recruitment of Zfp423 in one pathway appears to antagonize alternative pathways [4, 6], suggesting that Zfp423 may act to integrate competing signals into a canalized cellular response. Indeed, Zfp423 is a potent factor for embryonic stem cell exit from naïve state [8] and Zfp423 architecture and sequence are highly conserved [9].

Zfp423-mutant mice have characteristic developmental abnormalities, particularly in hindbrain. Loss of cerebellar vermis and other midline defects in developing brain are prominent features across independent null and hypomorphic alleles [10-12]. Vermis hypoplasia originates in reduced numbers of proliferating progenitors adjacent to the midline [10] and Zfp423 in cerebellar granule cell progenitors (GCPs) is required for mitogenic response to SHH signaling, potentially through repression of Tulp3 [13]. Development of the roof plate and choroid plexus in the fourth ventricle are frequently abnormal [10, 14]. Formation

of hippocampus, septum and thalamus are often affected, as are several fiber tracts, including frequent loss of midline crossing by commissural axons in corpus callosum and reduction of the anterior commissure [10, 11]. Loss of Zfp423 impairs maturation of olfactory neurons in a manner consistent with it acting in a developmental switch between early differentiating and maturing olfactory neurons [1]. Zfp423 is also expressed by preadipocyte fibroblasts, where it induces PPARg-dependent adipogenesis, and loss of *Zfp423* function impairs adipogenesis both in development [15] and in wound healing [16].

Mutations in the human homolog *ZNF423* have been reported in patients with ciliopathy diagnoses and anatomical findings reminiscent of *Zfp423* mutant mice [7] and a subset of patient mutations has been validated in mouse models [17]. Ciliopathies comprise a spectrum of related phenotypes that involve one or more organs, often cerebellum, kidney, retina, and/or liver, and are united by cellular defects in structure of and signaling through the primary cilium [18-20]. Ciliopathies also range in severity from nearly unaffected to prenatal lethal. Some of the differences arise from differences between causal genes or allele strength, but similar primary mutations can give rise to very different outcomes in both patients and mouse models depending on other genes and non-genetic factors [21, 22]. In previous work, we showed that differences in cerebellar hypoplasia had both genetic and non-genetic components in BALB/c and 129S1 strains [23], but the distribution and effect sizes of genetic modifiers and other sources of variability are not well explored.

Here, we show complete lethality of *Zfp423* mutants in a C57BL/6 background that correlates with both adiposity and neonatal feeding, and that lethality is specific to the perinatal period. As a prologue to both modeling patient mutations in mice and identifying modifiers that influence Zfp423-deficient developmental outcomes, we surveyed 13 inbred mouse strains through a series of (C57BL/6J–*Zfp423*^{nur12} x strain) x C57BL/6J–*Zfp423*^{nur12} backcrosses. Surprisingly, even C58, C57L, and C57BLKS, strains closely related to C57BL/6J, were able to support a modest number of surviving pups, some to a year or more of age. Calculated survival rates range from 8% to 95% depending on the strain pairing. Legacy data from earlier C57BL/6J–*Zfp423*^{nur12} x BALB/c intercross and backcross mice allowed us to infer a modifier locus on chromosome 5, explaining a fraction of survival differences between those strains.

Results

Zfp423 null allele is perinatal lethal in C57BL/6J strain background.

We examined *Zfp423*$^{nur12/+}$ mice as congenic lines on three common inbred strain backgrounds and as hybrids between them. Offspring were genotyped at 1 to 2 weeks. While *Zfp423*$^{nur12/nur12}$ showed somewhat reduced frequency in BALB/cAnNHsd (BALB) and 129S1/SvImJ (129S1) congenic strains, *Zfp423*$^{nur12/nur12}$ mice were never recovered among the C57BL/6J (B6) strain (Table 1). When B6–*Zfp423*$^{nur12/+}$ mice were crossed to BALB–*Zfp423*$^{nur12/+}$ mice,

the frequency of *Zfp423*^{nur12} homozygotes was consistent with full survival. The difference in homozygote frequency between BALB congenic stock and the BALB x B6 F1 (*P* = 0.019, Fisher's exact test) suggests that both strains contribute recessive alleles that reduce *Zfp423*$^{nur12/nur12}$ viability.

Table 1: *Zfp423*^{nur12} genotype frequencies (proportions) show enhanced lethality in B6 background.

Genotype	129S1-*nur12* F1	BALB-*nur12* F1	B6-*nur12* F1	BALB-*nur12* x B6-*nur12* F1
+/+	124 (0.31)	156 (0.28)	156 (0.35)	28 (0.24)
n/+	223 (0.56)	297 (0.53)	285 (0.65)	55 (0.47)
n/n	48 (0.12)	110 (0.20)	0 (0.00)	35 (0.30)
total	395	563	441	118
Chi-sq *P* for frequency n/n	3.7e-09	0.0035	(<2.2e-16)	0.24

To determine lethal periods and rule out segregation distortion or gametic effects, timed embryos and postnatal pups were collected and genotyped to determine the frequency of *Zfp423*^{nur12} homozygotes at each age. Only two mutants were observed at P1 and neither survived to P2. These data show complete perinatal lethality of *Zfp423*^{nur12} homozygotes on the B6 congenic background (Table 2).

Table 2: Genotype frequencies (proportions) by age support two lethal phases.

genotype	E12.5	E14.5	E16.5	E18.5	P0	P1
+/+	27 (0.20)	25 (0.21)	17 (0.22)	35 (0.26)	59 (0.29)	22 (0.30)
n/+	76 (0.55)	62 (0.53)	40 (0.51)	77 (0.57)	108 (0.54)	49 (0.67)
n/n	34 (0.25)	31 (0.26)	21 (0.27)	23 (0.17)	33 (0.16)	2 (0.027)
total	137	118	78	135	200	73
Chi-sq *P* for frequency n/n	0.96	0.75	0.69	0.032	0.005	1.2e-05

Fisher's exact *P* for comparison to previous day	-	0.89	1	0.11	0.76	0.0017

Reduced feeding and brown adipose tissue in B6–*Zfp423* neonates

To identify possible causes of lethality in B6-*Zfp423*$^{nur12/nur12}$ mice, we examined histology of P0 pups (Figure 2). Heart, kidney, and liver did not show any obvious defects. Sections through stomach show reduced amount of milk in B6 compared to BALB mice, independent of *Zfp423* genotype, while *Zfp423*$^{nur12/nur12}$ mice have reduced amount of milk compared to littermate controls in each strain, such that B6–*Zfp423*$^{nur12/nur12}$ mice are least well fed among comparison groups. Examination of brown adipose tissue confirmed small fat pads with gaps in the B6-*Zfp423*$^{nur12/nur12}$ mice as expected [15]. Two out of the three BALB-*Zfp423*$^{nur12/nur12}$ mice examined have normal brown adipose appearance, however, suggesting a degree of strain-dependence for this phenotype in limited sampling.

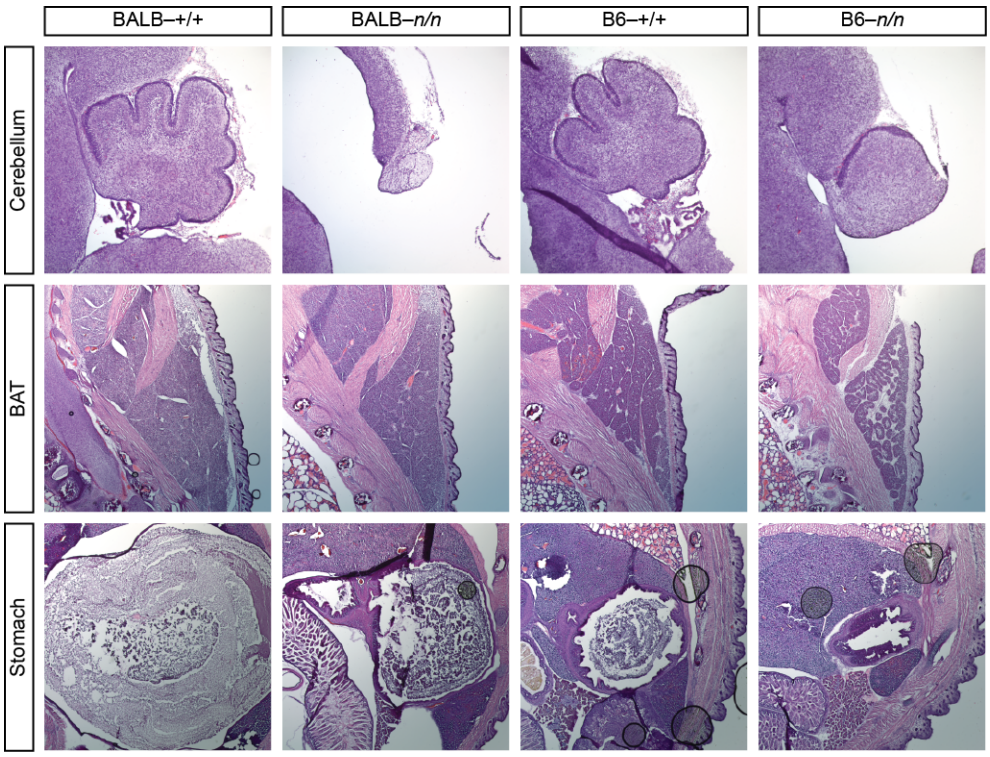

Figure 1. Histological differences between strains at P0. Typical images from a small series of P0 animals. *Zfp423*$^{nur12/nur12}$ homozygotes on both BALB and B6 backgrounds showed cerebellar vermis hypoplasia, anterior rotation and reduction or absence of choroid plexus. Brown adipose tissue generally appeared intact on BALB but reduced and less compact on B6. Stomach content was reduced in mutants, especially on B6 background.

B6 background enhances phenotype of a *Zfp423* hypomorphic allele.

To determine whether strain background might similarly affect weaker *Zfp423* alleles, we examined congenic lines for a hypomorphic gene trap line, XH542, that expresses ≤50% normal *Zfp423* RNA levels [10], on both BALB and B6 backgrounds (Figure 2). Gene trap homozygotes are viable on both backgrounds, but occur with reduced frequency on B6 (15% vs 26%, Figure 2A).

Surviving B6 gene trap homozygotes also have higher frequency of ataxia (Figure 2B). Gene trap homozygotes on both strain backgrounds had reduced cross-sectional area in vermis, but the difference between strains was not significant at conventional alpha for pre-planned sample size (N=11 paired samples, Figure 2C). Among samples allocated to anatomy we observed four with hydrocephalus, all of which were B6 gene trap homozygotes (Figure 2D). Taken together, these observations further support B6 as a sensitized background for loss of *Zfp423* function.

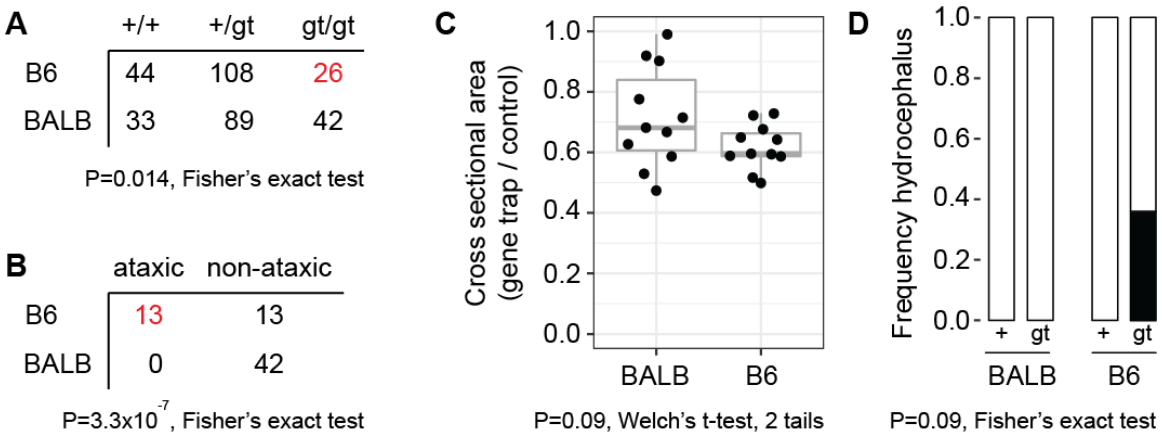

Figure 2. Congenic gene trap lines support B6 sensitivity to reduced Zfp423 function. (A) Gene trap (gt) homozygotes are recovered with reduced frequency on B6 but not BALB congenic background. (B) Surviving B6-gene trap homozygotes were frequently judged ataxic prior to genotyping, while BALB-gene trap homozygotes were not. (C) Parasagittal sections through cerebellar vermis showed reduced area in gene trap homozygotes compared to littermates, but the trend toward larger difference on B6 was not significant at alpha = 0.05 level for a two-tailed test. (D) A subset of B6 gene trap homozygotes were hydrocephalic, while none of the other mice were.

B6 sensitivity to *Zfp423* relative to BALB/c is polygenic, recessive in aggregate, and includes a locus on chromosome 5.

To test the genetic architecture of the striking difference in *Zfp423* survival and phenotype severity, we analyzed data from both B6 x BALB intercross and backcross designs performed several years ago. We specified linkage thresholds for suggestive (expected once per genome by chance) and significant (once in twenty genomes by chance) for a given cross design in advance [24] and assessed both marker-based chi-squared tests for proportion of B6 homozygotes at ascertainment (~2 weeks postnatal) and for survival up to P60 as a quantitative trait. In the intercross, chi-squared tests for proportion of B6 homozygotes (1 degree of freedom) supported linkage at genome-wide significance for reduced B6 homozygotes at a locus on chromosome 5 (P = 3.1 x 10^{-4} at rs254857227), with significant over-representation of B6 homozygotes on chromosome 13 (P = 3.7 x 10^{-4} at D13Mit17; Figure 3A). Similar analysis of an earlier intercross from a partially inbred stock had shown additional strong signals on chromosomes 11 and 17 that were not replicated in the intercross from fully congenic stocks, although the chromosome 17 locus remained significant in a combined analysis. This suggested context dependence and potential for epistatic interactions and resulted in limiting formal analysis to crosses initiated from fully congenic stocks. Analysis of a smaller backcross showed only suggestive levels of support for a locus on chromosome 12 (P = 0.0012) and sub-threshold support for the locus on chromosome 5 (P = 0.01), but

encompassing the same chromosome 5 interval as the intercross (Figure 3B). Selective genotyping of ~70 backcross progeny from other strain partners (see below) for survival at two weeks increased support for the chromosome 5 locus, with combined support across all backcrosses in the suggestive range (P = 6.9 x 10^{-4} at D5Mit157) for backcross data alone.

Most animals from both intercross and backcross populations also had survival data to postnatal day 60, which allowed use of a 2-part model for survival duration as a quantitative trait [25, 26]. Analysis of the intercross again showed significant linkage to the middle of chromosome 5, while also finding suggestive linkage on several other chromosomes (Figure 3C). Similar analysis of survival data from the backcross showed suggestive support for four regions, with strongest support for the chromosome 5 locus. In addition, the backcross animals that survived to at least P60 had significant depletion of B6 homozygotes compared to heterozygotes (22 vs. 59, chi-squared P = 3.9 x 10^{-5} at D5Mit398-D5Mit157) and was the most significant finding genome-wide for survival to P60. Two-part survival analysis combining the intercross and backcross data (for loci that might act independently in both contexts) showed strongest support was for the chromosome 5 locus (lod.p.mu = 7.4) with significant support for a locus on chromosome 6 (lod.p.mu = 5.1). Both loci were significant at genome-wide alpha < 0.02 based on 5000 permutations of the data. Effect plots for intercross (Figure 3E) and backcross (Figure 3F) showed that both loci reduce the probability of death at 3-5 weeks in favor of survival to the censored time point at P60.

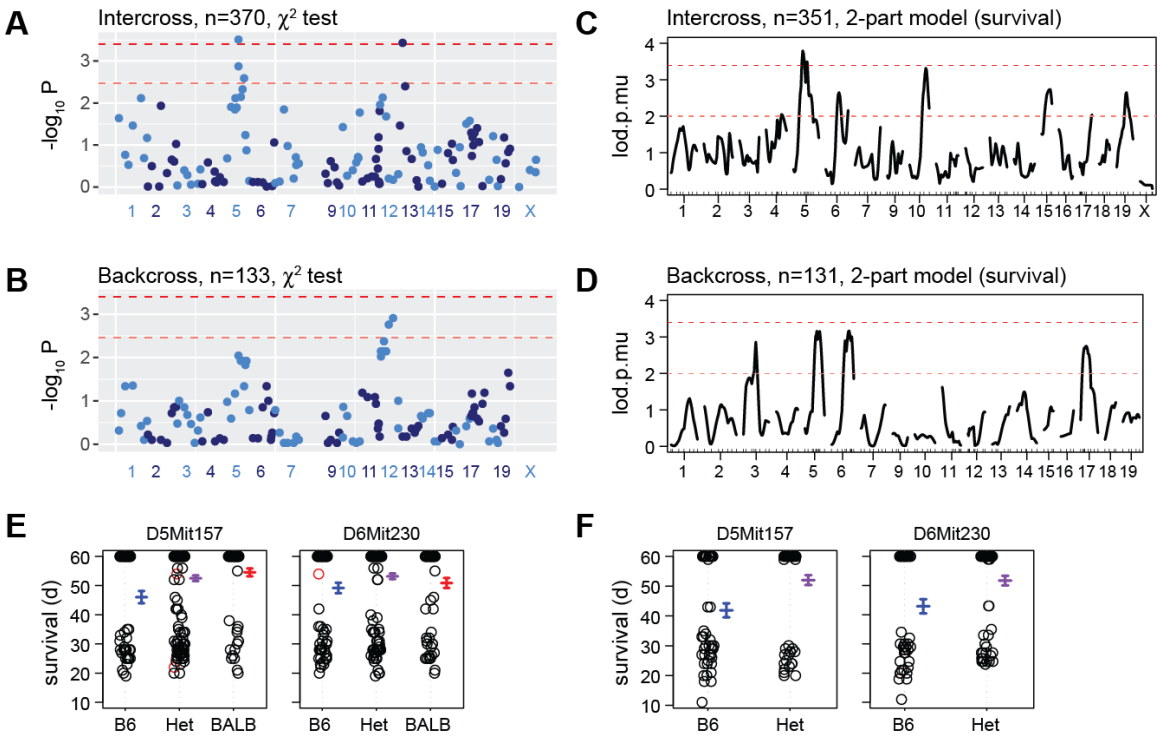

Figure 3. Linkage mapping supports a survival locus on Chr. 5. (A) Chi-squared tests for expected 25% B6-homozygous fraction (1 degree of freedom) in 370 F2 progeny from a BALB x B6 intercross. Chromosome 8 is omitted as constrained by *Zfp423* requirement. (B) Chi-squared test for 50% homozygotes in 133 backcross progeny. (C) 2-part model for survival (latency) up to P60 for the intercross progeny in (A). Lod.p.mu is the combined lod score for penetrance (lod.p) and severity (lod.mu) using log survival from entry at P12 to endpoint at P60 as a quantitative phenotype. (D) 2-part model applied to the backcross progeny in (B). (E) Marker effect plots for survival up to postnatal day (d) 60 in the intercross. (F) Effect plots for the same markers in the backcross.

B6 synthetic lethality is recessive rescued by any of 13 strain partners.

To examine the viability effects of strain background more broadly and to identify strains that might be useful for testing patient variants in an animal model, we crossed B6–*Zfp423*$^{nur12/+}$ to broad panel of inbred strains (Figure 4A) and then backcrossed the resulting F1 progeny to B6–*Zfp423*$^{nur12/+}$ to produce F2 (Figure 4B). Each strain partner produced viable mutant offspring, regardless of which sex was used as the F1 for backcross. The survival difference can not, therefore, be explained by B6 maternal behavior. Progeny of each cross were genotyped for *nur12* and all identified homozygotes had clearly recognized gait ataxia, indicating full penetrance. While some strains were under-sampled due to poor breeding performance, clear differences emerged among partner strains (Figure 4C). The frequency of F2 mutants recovered from the PWK/PhJ cross was 24% and not significantly different from Mendelian expectation (P = 0.84, chi-squared test, 1 df). By contrast, every other backcross showed reduced recovery, from 13% in 129S1/SvImJ ($P = 2.8 \times 10^{-5}$), to 2.5% in BTBR ($P = 1.5 \times 10^{-8}$). These data showed that survival of *Zfp423*^{nur12} homozygous mice is polygenic, with different sets of survival factors in different inbred stains.

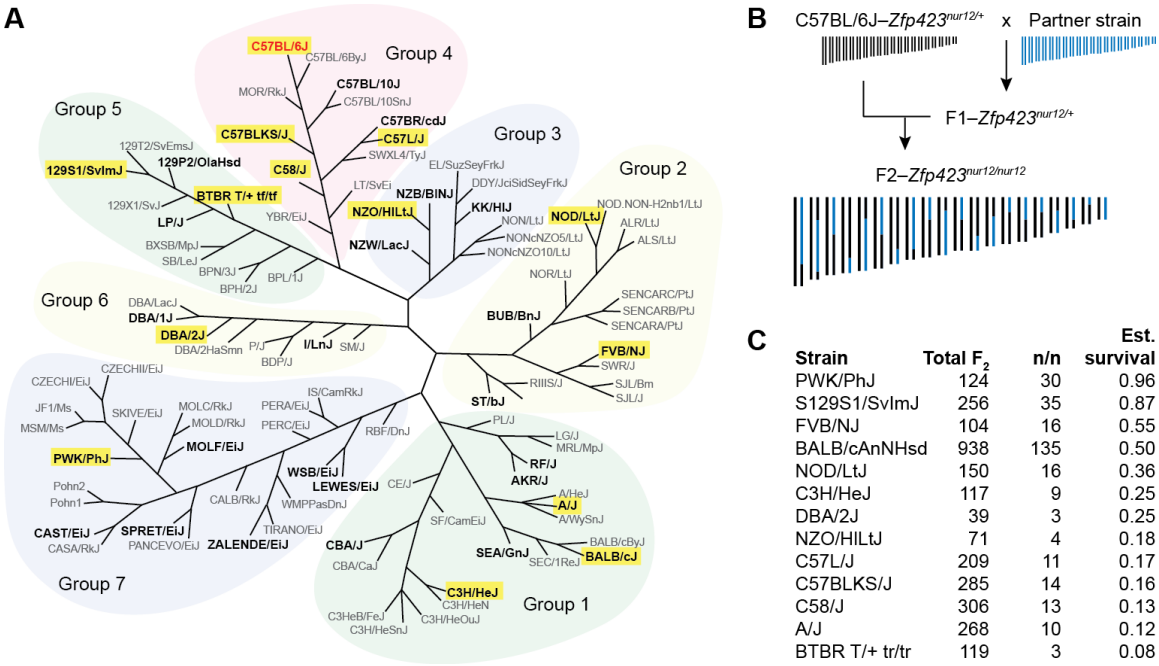

Strain	Total F_2	n/n	Est. survival
PWK/PhJ	124	30	0.96
S129S1/SvImJ	256	35	0.87
FVB/NJ	104	16	0.55
BALB/cAnNHsd	938	135	0.50
NOD/LtJ	150	16	0.36
C3H/HeJ	117	9	0.25
DBA/2J	39	3	0.25
NZO/HILtJ	71	4	0.18
C57L/J	209	11	0.17
C57BLKS/J	285	14	0.16
C58/J	306	13	0.13
A/J	268	10	0.12
BTBR T/+ tr/tr	119	3	0.08

Figure 4. Thirteen diverse strains rescue B6–*Zfp423*$^{nur12/+}$ lethality. (A) SNP-derived neighbor-joining tree modified from Petkov et al. [27]. Strains with public genome sequences [28] are in bold, strains tested for rescue of B6-dependent lethality highlighted with yellow rectangle. Only C57BL/6J (red, top) showed complete lethality. (B) Outcross-backcross design tests for dominant (or semi-dominant) effects. (C) Survival fraction was estimated as the number of *Zfp423*^{nur12} homozygotes divided by one-third the number of non-mutant offspring from the same cross.

Discussion

Our results showed that the *Zfp423*^{nut12} null allele is a fully penetrant perinatal lethal on a C57BL/6J (B6) genetic background, but has ≥50% survival when congenic on either 129S1 or BALB. Of the few neonates available for

examination, mutants on the B6 background appeared to have more severe peripheral tissues abnormalities compared with mutants congenic on BALB, including notably reduced adipose tissue and poor feeding. These observations are consistent with previous reports on Zfp423 requirements for adipocyte differentiation [15, 16, 29, 30] and suggest that this phenotype in vivo may be strain-dependent in its effect size. Greater sensitivity of B6 than BALB for loss of *Zfp423* function was supported by a small series of congenic mutants for a hypomorphic gene trap allele. Both survival and behavioral ataxia were substantially more penetrant on B6 than BALB, although statistical support for anatomical differences were sub-threshold and likely underpowered relative to the observed variance. This strain difference in sensitivity contrasts with recent work in our lab comparing different alleles on a single inbred background, where anatomical differences were more sensitive than behavior in a more extensive series of animals [17]. Surviving *Zfp423*^{nur12} mutants from intercross and backcross designs reported here showed that no single locus is either necessary or sufficient for mutant survival, but taken together, our results supported the existence of a modifier locus on chromosome 5, with suggestive or significant support for linkage at other loci being cross-dependent. Comparing survival rates among B6 backcross progeny from several different partner strains indicated different sets of pro-survival factors in different inbred strains. This suggests that searches for survival loci might be more powerful in strains with low survival frequency and close relation to B6, as these should limit the number of contributing loci and therefore the statistical power per surviving mutant. These

results also informed our choice of strains for modeling patient variants of uncertain significance [17], where FVB provided a high-survival, yet fully-penetrant background compatible with recovery of severe alleles and B6 provided a sensitized background to increase confidence in negative findings [17].

Materials and Methods

Mice. Congenic *Zfp423*^{nur12} and *Zfp423*^{XH542} mice were developed by serial backcross from mixed stock [10, 23]. Linked markers on chromosome 8 were followed in early generations to minimize linked variation. BALB/cAnNHsd was obtained through the UC San Diego Transgenic Mouse Shared Resource and maintained in our laboratory. PWK mice were obtained from Dr. Christopher K. Glass. All other strains were obtained from The Jackson Laboratory. Crosses and offspring were maintained on LabDiet 5P06 chow ad libitum and a 12:12 hour light:dark cycle in microisolator cages on high-density racks in a specific pathogen free facility.

Linkage analysis. Marker loci were tested for reduced frequency of C57BL/6J allele homozygosity among surviving *Zfp423*^{nur12} homozygous pups using a chi-squared test in the R base environment using genotype frequencies tabulated in R/qtl [31, 32]. Tests for duration of survival, up to 60 days, was carried out using the 2-step procedure in R/qtl scanone function [25, 26].

Acknowledgements

We thank Professor Christopher K. Glass for the gift of PWK/PhJ breeders. We thank Wilfredo Villanueva and Abraham Ramirez for excellent animal care. W.A.A. was supported in part by an institutional training grant to the UC San Diego Genetics Training Program (T32 GM008666) from the National Institute of General Medical Sciences and by a Ruth L. Kirschstein National Research Service Award (F31 NS061513) from the National Institute of Neurological Disorders and Stroke. This work was supported by grants R01 NS054871 and R01 NS097534 from the National Institute of Neurological Disorders and Stroke to B. A. H.

References

1. Cheng LE, Reed RR. Zfp423/OAZ participates in a developmental switch during olfactory neurogenesis. Neuron. 2007;54(4):547-57. doi: 10.1016/j.neuron.2007.04.029. PubMed PMID: 17521568; PubMed Central PMCID: PMCPMC2866517.

2. Tsai RY, Reed RR. Cloning and functional characterization of Roaz, a zinc finger protein that interacts with O/E-1 to regulate gene expression: implications for olfactory neuronal development. J Neurosci. 1997;17(11):4159-69. PubMed PMID: 9151733.

3. Tsai RY, Reed RR. Identification of DNA recognition sequences and protein interaction domains of the multiple-Zn-finger protein Roaz. Mol Cell Biol. 1998;18(11):6447-56. doi: 10.1128/mcb.18.11.6447. PubMed PMID: 9774661; PubMed Central PMCID: PMCPMC109231.

4. Hata A, Seoane J, Lagna G, Montalvo E, Hemmati-Brivanlou A, Massague J. OAZ uses distinct DNA- and protein-binding zinc fingers in separate BMP-Smad and Olf signaling pathways. Cell. 2000;100(2):229-40. doi: 10.1016/s0092-8674(00)81561-5. PubMed PMID: 10660046.

5. Huang S, Laoukili J, Epping MT, Koster J, Holzel M, Westerman BA, et al. ZNF423 is critically required for retinoic acid-induced differentiation and is a marker of neuroblastoma outcome. Cancer Cell. 2009;15(4):328-40. doi: 10.1016/j.ccr.2009.02.023. PubMed PMID: 19345331; PubMed Central PMCID: PMCPMC2693316.

6. Masserdotti G, Badaloni A, Green YS, Croci L, Barili V, Bergamini G, et al. ZFP423 coordinates Notch and bone morphogenetic protein signaling, selectively up-regulating Hes5 gene expression. J Biol Chem. 2010;285(40):30814-24. doi: 10.1074/jbc.M110.142869. PubMed PMID: 20547764; PubMed Central PMCID: PMCPMC2945575.

7. Chaki M, Airik R, Ghosh AK, Giles RH, Chen R, Slaats GG, et al. Exome capture reveals ZNF423 and CEP164 mutations, linking renal ciliopathies to DNA damage response signaling. Cell. 2012;150(3):533-48. doi: 10.1016/j.cell.2012.06.028. PubMed PMID: 22863007; PubMed Central PMCID: PMCPMC3433835.

8. Lackner A, Sehlke R, Garmhausen M, Stirparo GG, Huth M, Titz-Teixeira F, et al. Cooperative molecular networks drive a mammalian cell state transition. bioRxiv. 2020:2020.03.23.000109. doi: 10.1101/2020.03.23.000109.

9. Hamilton BA. ZNF423 orthologs are highly constrained in vertebrates but show domain-level plasticity across invertebrate lineages. bioRxiv. 2020:2020.03.09.984518. doi: 10.1101/2020.03.09.984518.

10. Alcaraz WA, Gold DA, Raponi E, Gent PM, Concepcion D, Hamilton BA. Zfp423 controls proliferation and differentiation of neural precursors in cerebellar vermis formation. Proc Natl Acad Sci U S A. 2006;103(51):19424-9. doi: 10.1073/pnas.0609184103. PubMed PMID: 17151198; PubMed Central PMCID: PMCPMC1748242.

11. Cheng LE, Zhang J, Reed RR. The transcription factor Zfp423/OAZ is required for cerebellar development and CNS midline patterning. Dev Biol. 2007;307(1):43-52. doi: 10.1016/j.ydbio.2007.04.005. PubMed PMID: 17524391; PubMed Central PMCID: PMCPMC2866529.

12. Warming S, Rachel RA, Jenkins NA, Copeland NG. Zfp423 is required for normal cerebellar development. Mol Cell Biol. 2006;26(18):6913-22. doi: 10.1128/MCB.02255-05. PubMed PMID: 16943432; PubMed Central PMCID: PMCPMC1592861.

13. Hong CJ, Hamilton BA. Zfp423 Regulates Sonic Hedgehog Signaling via Primary Cilium Function. PLoS Genet. 2016;12(10):e1006357. doi: 10.1371/journal.pgen.1006357. PubMed PMID: 27727273; PubMed Central PMCID: PMCPMC5065120.

14. Casoni F, Croci L, Vincenti F, Podini P, Massimino L, Cremona O, et al. ZFP423 regulates early patterning and multiciliogenesis in the hindbrain choroid plexus. bioRxiv. 2020:2020.03.04.975573. doi: 10.1101/2020.03.04.975573.

15. Gupta RK, Arany Z, Seale P, Mepani RJ, Ye L, Conroe HM, et al. Transcriptional control of preadipocyte determination by Zfp423. Nature. 2010;464(7288):619-23. doi: 10.1038/nature08816. PubMed PMID: 20200519; PubMed Central PMCID: PMCPMC2845731.

16. Plikus MV, Guerrero-Juarez CF, Ito M, Li YR, Dedhia PH, Zheng Y, et al. Regeneration of fat cells from myofibroblasts during wound healing. Science. 2017;355(6326):748-52. doi: 10.1126/science.aai8792. PubMed PMID: 28059714; PubMed Central PMCID: PMCPMC5464786.

17. Deshpande O, Lara RZ, Zhang OR, Concepcion D, Hamilton BA. ZNF423 patient variants, truncations, and in-frame deletions in mice define an allele-dependent range of midline brain abnormalities. bioRxiv. 2020:2020.04.04.024562. doi: 10.1101/2020.04.04.024562.

18. Badano JL, Mitsuma N, Beales PL, Katsanis N. The ciliopathies: an emerging class of human genetic disorders. Annu Rev Genomics Hum Genet. 2006;7:125-48. Epub 2006/05/26. doi: 10.1146/annurev.genom.7.080505.115610. PubMed PMID: 16722803.

19. Hildebrandt F, Benzing T, Katsanis N. Ciliopathies. The New England journal of medicine. 2011;364(16):1533-43. Epub 2011/04/22. doi: 10.1056/NEJMra1010172. PubMed PMID: 21506742.

20. Waters AM, Beales PL. Ciliopathies: an expanding disease spectrum. Pediatr Nephrol. 2011;26(7):1039-56. Epub 2011/01/07. doi: 10.1007/s00467-010-1731-7. PubMed PMID: 21210154; PubMed Central PMCID: PMC3098370.

21. Davis EE, Katsanis N. The ciliopathies: a transitional model into systems biology of human genetic disease. Curr Opin Genet Dev. 2012;22(3):290-303. Epub 2012/05/29. doi: 10.1016/j.gde.2012.04.006. PubMed PMID: 22632799; PubMed Central PMCID: PMC3509787.

22. Norris DP, Grimes DT. Mouse models of ciliopathies: the state of the art. Dis Model Mech. 2012;5(3):299-312. Epub 2012/05/09. doi: 10.1242/dmm.009340. PubMed PMID: 22566558; PubMed Central PMCID: PMC3339824.

23. Alcaraz WA, Chen E, Valdes P, Kim E, Lo YH, Vo J, et al. Modifier genes and non-genetic factors reshape anatomical deficits in Zfp423-deficient mice. Hum Mol Genet. 2011;20(19):3822-30. doi: 10.1093/hmg/ddr300. PubMed PMID: 21729880; PubMed Central PMCID: PMCPMC3168291.

24. Lander E, Kruglyak L. Genetic dissection of complex traits: guidelines for interpreting and reporting linkage results. Nat Genet. 1995;11(3):241-7. doi: 10.1038/ng1195-241. PubMed PMID: 7581446.

25. Boyartchuk VL, Broman KW, Mosher RE, D'Orazio SE, Starnbach MN, Dietrich WF. Multigenic control of Listeria monocytogenes susceptibility in mice. Nat Genet. 2001;27(3):259-60. doi: 10.1038/85812. PubMed PMID: 11242105.

26. Broman KW. Mapping quantitative trait loci in the case of a spike in the phenotype distribution. Genetics. 2003;163(3):1169-75. PubMed PMID: 12663553; PubMed Central PMCID: PMCPMC1462498.

27. Petkov PM, Ding Y, Cassell MA, Zhang W, Wagner G, Sargent EE, et al. An efficient SNP system for mouse genome scanning and elucidating strain relationships. Genome Res. 2004;14(9):1806-11. doi: 10.1101/gr.2825804. PubMed PMID: 15342563; PubMed Central PMCID: PMCPMC515327.

28. Keane TM, Goodstadt L, Danecek P, White MA, Wong K, Yalcin B, et al. Mouse genomic variation and its effect on phenotypes and gene regulation. Nature. 2011;477(7364):289-94. doi: 10.1038/nature10413. PubMed PMID: 21921910; PubMed Central PMCID: PMCPMC3276836.

29. Gupta RK, Mepani RJ, Kleiner S, Lo JC, Khandekar MJ, Cohen P, et al. Zfp423 expression identifies committed preadipocytes and localizes to adipose endothelial and

perivascular cells. Cell Metab. 2012;15(2):230-9. doi: 10.1016/j.cmet.2012.01.010. PubMed PMID: 22326224; PubMed Central PMCID: PMCPMC3366493.

30. Shao M, Hepler C, Vishvanath L, MacPherson KA, Busbuso NC, Gupta RK. Fetal development of subcutaneous white adipose tissue is dependent on Zfp423. Mol Metab. 2017;6(1):111-24. doi: 10.1016/j.molmet.2016.11.009. PubMed PMID: 28123942; PubMed Central PMCID: PMCPMC5220400.

31. Broman KW, Sen S. A Guide to QTL Mapping with R/qtl. M. G, Krickberg K, Samet J, Tsiatis A, Wong W, editors. Dordrecht: Springer; 2009. 396 p.

32. Broman KW, Wu H, Sen S, Churchill GA. R/qtl: QTL mapping in experimental crosses. Bioinformatics. 2003;19(7):889-90. Epub 2003/05/02. PubMed PMID: 12724300.